frontiers in Marine Science

ORIGINAL RESEARCH
published: 17 November 2017
doi: 10.3389/fmars.2017.00365

# Use of Open Source Hardware and Software Platforms to Quantify Spectrally Dependent Differences in Photochemical Efficiency and Functional Absorption Cross Section within the Dinoflagellate *Symbiodinium* spp.

*Kenneth D. Hoadley*[*†] *and Mark E. Warner*

*School of Marine Science and Policy, University of Delaware, Lewes, DE, United States*

OPEN ACCESS

**Edited by:**
*Thomas K. Frazer, University of Florida, United States*

**Reviewed by:**
*Bojan Tamburic, University of Technology Sydney, Australia*
*Oscar Schofield, Rutgers University, The State University of New Jersey, United States*

***Correspondence:**
*Kenneth D. Hoadley*
*khoadley@mbari.org*

**†Present Address:**
*Kenneth D. Hoadley, Monterey Bay Aquarium Research Institute. Moss Landing, CA, United States*

**Specialty section:**
*This article was submitted to Coral Reef Research, a section of the journal Frontiers in Marine Science*

**Received:** *18 May 2017*
**Accepted:** *30 October 2017*
**Published:** *17 November 2017*

**Citation:**
*Hoadley KD and Warner ME (2017) Use of Open Source Hardware and Software Platforms to Quantify Spectrally Dependent Differences in Photochemical Efficiency and Functional Absorption Cross Section within the Dinoflagellate Symbiodinium spp. Front. Mar. Sci. 4:365. doi: 10.3389/fmars.2017.00365*

Active chlorophyll *a* fluorescence is an essential tool for understanding photosynthetic activity within cnidarian/dinoflagellate symbioses. Fluorescence measurement is typically achieved by utilizing a blue or red monochromatic excitation light source. However, algal photosynthetic pigments can differ in their absorption spectra, potentially leading to excitation wavelength dependent measurements of maximal and light acclimated PSII photosynthetic quantum yield (Fv/Fm or Fq′/Fm′) and functional absorption cross section ($\sigma_{PSII}$ or $\sigma_{PSII'}$). Here we utilized an open source hardware development platform to construct a multispectral excitation fluorometer to assess spectrally dependent differences in photochemistry within four different *Symbiodinium* species (two of each ITS2-type A4 and B1). Multivariate analysis of light acclimated photochemical signatures showed separation between most alga types. These spectrally dependent differences in light acclimated PSII efficiency and PSII functional absorption cross section likely reflect changes in light harvesting compounds, their connectivity to the PSII reaction centers and the balance between photochemical and non-photochemical fluorescence quenching. Additionally, acclimation to low (20 μmol photons $m^{-2}$ $s^{-1}$) and high (200 μmol photons $m^{-2}$ $s^{-1}$) light conditions was examined in two of these symbionts types (ITS-2 type A4 and B1) As expected, chlorophyll a $cell^{-1}$ decreased under high light acclimation in both symbionts. However, only A4 saw a subsequent reduction in absorbance whereas cellular volume decreased in the B1 (*S. minutum*) symbiont. In response to high light acclimation, Fv/Fm was significantly lower at all excitation wavelengths for the B1 symbiont where as efficiencies remained the same for A4. However, high-light acclimated Fq′/Fm′ levels decreased in both symbionts, but only when measured using the 615 or 625 nm excitation wavelengths. Non-photochemical quenching within the antennae bed was downregulated under high light acclimation in the A4 symbiont, but only when measured using the 505 and 530 nm excitation wavelengths. Such changes in Fq′/Fm′ and antennae bed quenching highlight the

benefits of spectrally resolved photochemical measurements. Additionally, the utilization of Arduino and Bitscope hardware exemplifies the potential of open source development platforms for construction of highly customizable instrumentation for photosynthetic research.

**Keywords: multispectral fluorometer, absorbance, light acclimation, open source, coral photobiology**

## INTRODUCTION

Dinoflagellates within the genus *Symbiodinium* can form unique symbioses with various marine invertebrate species, including jellyfish, sea anemones, giant clams, soft corals, and hard corals or scleractinians. These symbioses are pivotal for the ecological success of many of these organisms as they provide a major carbon source to their hosts via translocation of energy rich photosynthate (Muscatine et al., 1984; Muscatine, 1990). This genus contains a high degree of genetic diversity which is currently organized into nine broad clades (designated by the letters A–I), some of which contain hundreds of distinct species (LaJeunesse, 2001). Importantly, different *Symbiodinium*s can have significant influence on the host's response to changes in the environment (Baker, 2003). For example, in corals, thermal tolerance is often associated with the specific symbiont type (Kemp et al., 2006; LaJeunesse et al., 2009; Silverstein et al., 2011; Ortiz et al., 2012). However, matching physiological characteristics with specific symbiont types can be difficult and time consuming. There is a real need within the coral reef community to match physiological variability with genetic variance across symbiont types to better understand what/how these symbioses will respond under future climate conditions.

Such phenotypic assessment (Phenomics) is gaining momentum within other photobiological fields where comprehension of genetic variability has far outpaced phenotypic descriptions (Furbank and Tester, 2011). Phenotypic structure across different symbiont types grown in culture has been documented using photophysiological metrics as measured using active chlorophyll fluorometric measurements (Suggett et al., 2015). However, environmental variables such as light intensity and the spectral characteristics inherent to the coral host in which the symbiont resides can also influence photobiological behavior (Iglesias-Prieto and Trench, 1997b; Iglesias-Prieto et al., 2004; Wangpraseurt et al., 2012, 2014). The potential for phenotypic variance within a single species also increases the difficulty of matching physiology with genotype in symbiodinium (Iglesias-Prieto and Trench, 1997b; Iglesias-Prieto et al., 2004).

The genus *Symbiodinium* contains a number of different photopigments, some involved with light harvesting, while others act as accessory pigments where they can either channel additional energy toward the photosynthetic reaction centers, or dissipate excess light energy (Iglesias-Prieto and Trench, 1994, 1997b). The light harvesting compounds; peridinin-chlorophyll-a-protein (PCP) and chl a-chl c(2)-peridinin-protein (acpPC) have been particularly well-studied and comprise the primary light harvesting units within *Symbiodinium* (Iglesias-Prieto et al., 1991, 1993; Niedzwiedzki et al., 2013, 2014). The relative abundance of these different photopigments can differ across symbiont types (Hennige et al., 2009) and potentially offer another biological parameter that can be utilized to study species specific phenotypes within the genus *Symbiodinium.* As was demonstrated with symbionts housed within *Porites* and *Montipora,* host coral specimens found in Kaneohe Bay, absorbance based measurements can under certain circumstances provide some information on the abundance of photopigment concentrations (Hochberg et al., 2006). However, additional instrumentation is needed to understand the active role of these pigments within the photosynthetic apparatus.

Single turnover (ST) active chlorophyll-*a* fluorometers utilize a short (<300 μs) saturation light pulse to induce charge separation and reduction of the primary electron acceptor $Q_a$ within the PSII reaction center (Kolber and Falkowski, 1998). A major advantage of ST fluorometery is the additional measurement of the functional absorption cross section of PSII ($\sigma_{PSII}$) (Suggett et al., 2003), which measures the proportion of light captured by light harvesting proteins attached to a reaction center and utilized by PSII. In these instruments, saturation/excitation lamps are typically centered at a 450–500 nm wavelength to target peak absorbance of chlorophyll-*a*. However, by adjusting the excitation wavelength, it is possible to preferentially target other light harvesting photopigments. For example, by utilizing LEDs with peak emission centered at 447, 505 or 530 nm, we are able to preferentially excite at the peak absorption "soret" bands for the pigments Chl $a/c_2$, diadinoxanthin, and peridinin, respectively (Niedzwiedzki et al., 2013, 2014). Longer wavelengths such as 625 nm may transfer energy directly to the Chl *a* molecule (Niedzwiedzki et al., 2014). Preferential excitation may provide further insight into how pigment orientation and connectivity to the PSII reaction center may differ across environmental conditions or across symbiont types. However, such systems come at a high cost and alternative systems could be highly beneficial toward improving our understanding of *Symbiodinium* photobiology.

Hardware and software platforms designed to help teach coding and programming languages to the next generation of engineers are becoming increasingly popular within the scientific community. These platforms offer sophisticated microcontrollers as a base with which to design customized instrumentation at a low cost. The high cost of commercially available research instrumentation can be heavily restrictive to many laboratories. Research questions/initiatives often must cater to the available instrumentation, thereby limiting the scope of possible questions or experimental options. Open-sourced hardware and software platforms have the potential to revolutionize how scientists conduct research by allowing for cheap purpose built instrumentation. Sophisticated

instrumentation can be cheaply designed and built around a specific research question/topic. For example, the MultispeQ is an instrument developed to compare photophysiological parameters in plants across the world in an effort to tie in physiological differences with known genetic variance (Kuhlgert et al., 2016). The OpenROV project (www.openrov.com) represents another open-source platform which utilizes both the Arduino and Beaglebone hardware to construct a low cost remotely operated underwater vehicle which can be adapted with different instrumentation for both recreational and/or research purposes. These low-cost, yet highly sophisticated instruments represent an emerging trend in research that have great potential moving forward.

In this study, we utilize open source platforms to construct a low-cost multispectral ST fluorometer to characterize potential photo-physiological differences across four symbiont types from two clades (A and B) living within the anemone *Exaptasia pallida*. We further characterized the light acclimation process within two of these symbionts and describe a spectrally dependent response which differed across the *Symbiodinium* types. This study serves as an example of the potential for furthering scientific inquiry through customized, purpose built instruments via the open source concept and designed for specific research questions.

# MATERIALS AND METHODS

## Development of Host and Symbiont Combinations

Symbiont strain identification was determined through partial amplification of the ITS2 nuclear ribosomal DNA region and a region of the chloroplast 23S rDNA as described in LaJeunesse and Trench (2000) and Zhang et al. (2000). The two strains of ITS-2 type A4 utilized within this study were collected from *E. pallida* anemones in a mangrove habitat in Key Largo, FL (Hawkins et al., 2016). The A4-a strain represents a natural host and symbiont combination whereas the A4-b strain represents the genotype KLAp2 isolated from the anemone population and then utilized to re-infect aposymbiotic anemones originating from the same Key Largo mangrove habitat (as described in Hawkins et al., 2016). Both the B1-a and B1-b strains represent separate *S. minutum* genotypes and are housed within *E. pallida* (clone CC7, donated by J. Pringle, Stanford University) (Sunagawa et al., 2009). The B1-a strain represents a *S. minutum* variant that is naturally found within *E. pallida* and the B1-b strain was originally isolated from a Caribbean gorgonian (*Plexaura kuna*) (the BURR culture collection, donated by M.A. Coffroth, University of Buffalo). All host symbiont combinations were maintained in stable symbioses for at least 6 months prior to experimentation.

Each host/symbiont combination was maintained in small glass bowls (9 cm diameter, 130-mL volume) filled with artificial seawater (Instant Ocean) at a temperature of 26°C and salinity of 34 ppt. Lighting was maintained at 40 μmol photons $m^{-2}$ $s^{-1}$ with a 14:10 h light dark cycle using cool white fluorescent bulbs. Anemones were fed *Artemia nauplii* twice per week and seawater in each bowl was changed every 3 days.

## Experimental Conditions

For comparisons of spectrally dependent quantum yield and functional absorption cross section measurements across symbiont types, four different host/symbiont combinations (A4-a, A4-b, B1-a, and B1-b) were maintained in separate glass bowls with 3–4 anemones per bowl. Anemones were maintained at 20 μmol photons $m^{-2}$ $s^{-1}$ on a 14:10 h light:dark cycle. For spectrally dependent characterization across low and high light acclimated cells, additional bowls for A4-a and B1-a were kept at 200 μmol photons $m^{-2}$ $s^{-1}$ on a 14:10 h light:dark cycle. All bowls were cleaned and filled with fresh artificial seawater every 3 days and anemones were fed twice per week. Temperature was maintained at 26°C. Anemones were acclimated to their respective light conditions over a 2-week period prior to taking chlorophyll a fluorescence measurements and sampling anemones for chlorophyll a concentration, cell count, and cell volume measurements.

## Chlorophyll a Fluorescence Measurements

### Construction of Open-Sourced Fluorometer

The fluorometer prototype consists of combining several commercially available pieces of electronics. The Bitscope comes with a fully functional software program whereas the Arduino comes with its own code compiler. A schematic of the constructed fluorometer is provided in **Figure 1** and the components are listed in **Table 1**. In brief, excitation was achieved using CREE XLamp XP-E2 LED. Three LEDs wired in series on a metal core printed circuit board (MCPCB) were utilized per excitation color (Channel). Specific LED colors (447, 505, 530, 597, 615, and 625 nm) were chosen due to their commercial availability and for their overlap with peak photopigment absorption values (Niedzwiedzki et al., 2013, 2014). Excitation of each Channel was controlled using logic MOSFET transistors connected to separate IO pins on an Arduino UNO microcontroller board. Power to the LEDs was supplied by a 12-volt AC-DC power converter (Mean-Well). A voltage regulator controlled power to each LED. However, due to performance differences across the LED colors, irradiance differed across wavelengths (447 nm = 34,172; 505 nm = 16,209; 530 nm = 18,401; 597 nm = 24,089; 615 nm = 35,983; 625 nm = 43,662 μmol photons $m^{-2}$ $s^{-1}$). Although similar irradiance across all excitation wavelengths is ideal, such differences should not affect the calculation of absorption cross section so long as light levels are not so low as to allow for reoxidation of the $Q_A^-$ site within the PSII reaction center (Kolber and Falkowski, 1998). Excitation irradiance values were monitored throughout using an incident quantum sensor (LI-192, LiCor) to ensure stability throughout measurements. Fluorescence rise kinetics were detected with a PIN photodiode (Hammamatsu) connected to a LT122 operational amplifier (Linear Technology) along with a longband pass filter (Schott-RG695). The operational amplifier circuit came prefabricated as part of a Demonstration Circuit Board (1416; Linear Technology) and powered using a ± 15 volt DC-DC (CUI) power supply. The resulting analog output from the PIN photodiode was recorded using a 10AU pocket analyzer (Bitscope). Control of each excitation channel, and the trigger to record data with the

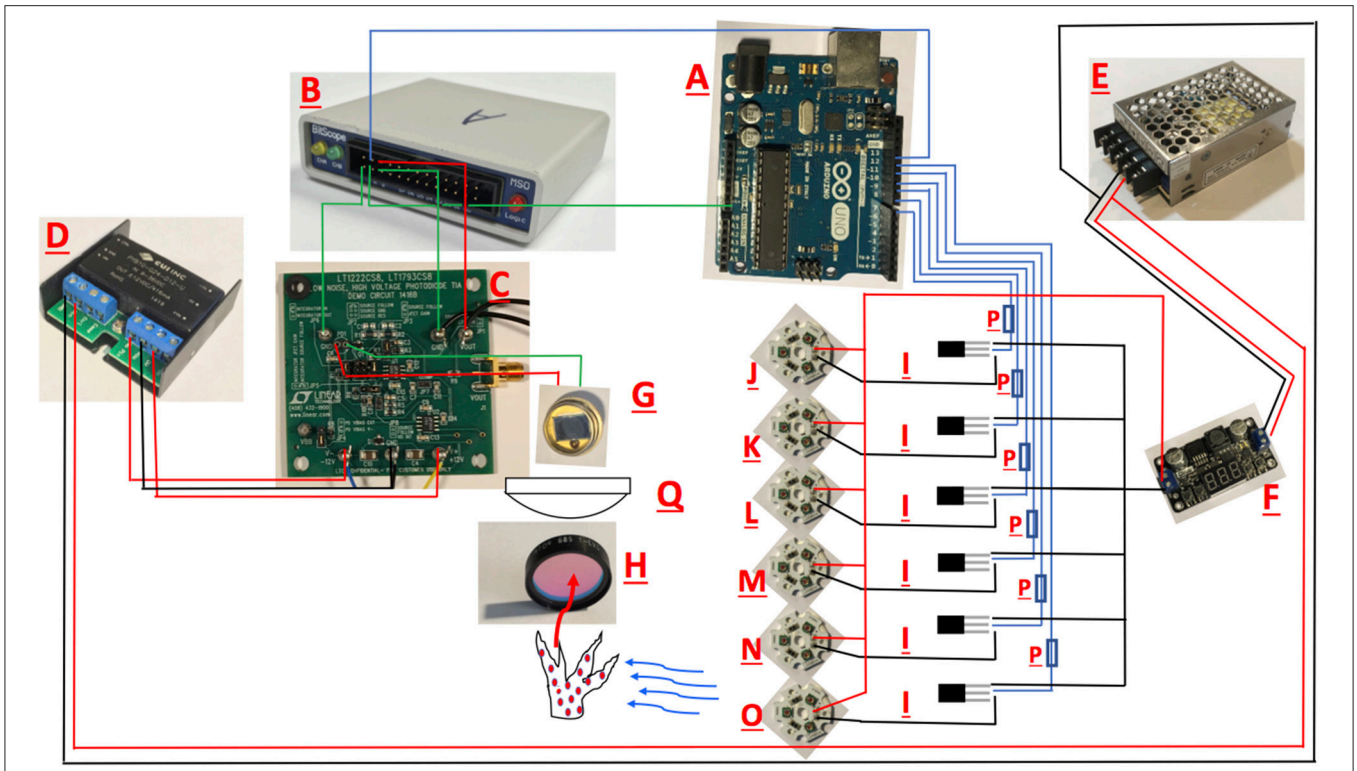


**FIGURE 1 |** Schematic for the open source multispectral fluorometer. Names of Individual parts are listed in **Table 1**. Black and red lines illustrate wire connections between hardware.

10 AU pocket analyzer was achieved using the Arduino IDE. The Arduino control script is available on github (https://github.com/khoadley/Fluorometer). Light emission and fluorescence detection were directed by glass fiber optic light guides (19.05-mm diameter) oriented at a 90-degree angle to each other.

Measurements were made 1 h after lights were turned off and consisted of six iterations of a 150 μs flash for each of the six excitation wavelengths. Light acclimated fluorescence measurements were then recorded following a 5-min exposure to a cool white actinic LED light source (CREE R5) at an intensity of 200 μmol photons $m^{-2}$ $s^{-1}$. Reference curves for each channel and light stage were recorded using a solid fluorescence standard (Walz). Fluorescence induction curves were processed in R with the non-linear curve (nlc) fitting package using equations adapted from Kolber and Falkowski (1998) by Dr. Matt Oliver (University of Delaware). Briefly, the data is fit to the equation:

$$F = F_{0EST} + F_{vEST}{}^{*}(1 - \exp(-(C^{*}x)/1))$$

Where $F_{0EST}$, $F_{vEST,}$ and C are derived through iterative curve fitting. $F_0$ and $F_m$ are equal to F at the initial and final time point within the curve, respectively. The functional absorption cross section is determined by dividing C by the light irradiance measured from the corresponding excitation LED (R script is also available via Github: https://github.com/khoadley/Fluorometer). The proportion of non-photochemical quenching which is occurring within the light harvesting pigments (non-photochemical quenching in the antennae bed) was calculated as 1-($\sigma_{PSII}$'/$\sigma_{PSII}$) where $\sigma'_{PSII}$ and $\sigma_{PSII}$ reflect the light and dark acclimated functional absorption cross section of PSII (Gorbunov et al., 2001; Hennige et al., 2009).

### Commercially Available Instrument

On the final sampling interval, the maximum quantum yield of photosystem II (PSII, Fv/Fm) and the functional absorption cross section of PSII ($\sigma_{PSII}$) were also measured using a fluorescence induction and relaxation (FIRe) fluorometer (Satlantic Inc., Halifax) (**Figure 6**). Measurements were taken 1 h after the start of the dark period and consisted of five iterations of a 120 μs single turnover flash and analyzed by fitting each fluorescence transient curve using the *FIREPRO* software (Kolber and Falkowski, 1998; Hennige et al., 2009).

## Algal Cell Number, Volume, and Chlorophyll a Concentration

Each anemone was ground in 1 mL of seawater using a 1.5 mL glass tenbroeck tissue grinder. A 200-μL sample of the resulting homogenate was removed and fixed with 10 μL 1% glutaraldehyde and used for algal cell counts and volume as described below. The remaining homogenate was centrifuged (5,000 × g) for 5 min to separate the host and symbiont portions. The supernatant was removed

**TABLE 1 |** Equipment list for fluorometer build.

| Letter | Hardware | Company | Description | Approximate Price (USD) |
|---|---|---|---|---|
| A | Arduino UNO | Arduino | Microcontroller | $24.95 |
| B | BitScope BS10 | BitScope | Oscilloscope | $245.00 |
| C | 1416A | Linear Tech | Photodiode amplifier | $70 |
| D | ± 15 vdc power source | CUI | DC-DC power converter | $30 |
| E | 24 vdc power source | Mean-Well | AC-DC Converter | $35 |
| F | Voltage Regulator | Drok | Voltage Regulator | $16.89 |
| G | PDB-C109-ND | Digi-Key | PIN photodiode | $71.60 |
| H | RG695 | Schott | Long Bandpass filter | $40 |
| I | IRL-520 | Vishay | MOSFET | <$2.00 each |
| J | XP-E (Royal Blue) | Cree LED | 447 nm Excitation | $15 |
| K | Luxeon Rebel (Blue) | Luxeon LED | 505 nm Excitation | $15 |
| L | XP-E (Green) | Cree LED | 530 nm Excitation | $15 |
| M | XP-E (Amber) | Cree LED | 597 nm Excitation | $15 |
| N | XP-E (Red Orange) | Cree LED | 615 nm Excitation | $15 |
| O | XP-E (Red) | Cree LED | 625 nm Excitation | $15 |
| P | | Digikey | Resistor | <$1 each |
| Q | Aspheric Lens | Newport | Aspheric condenser | 71 |
| | | | | Total: $712.44 |

*Figure letters correspond to* ***Figure 1****.*

for calculating host protein concentration. The remaining algal cell pellet was utilized for calculating chlorophyll a concentration. Algal cell density and volume was assessed by replicate hemocytometer counts ($n = 6$) under 100x magnification. Samples were photographed using a Nikon microphot-FXA epifluorescent microscope and then analyzed by computer using Image J software (NIH) using methods similar to Suggett et al. (2015). For photopigment quantification, pelleted cells were lysed in 90% methanol with a bead beater (BioSpec) for 60 s, incubated at −20°C for 2 h and then centrifuged for 5 min at 5,000 rpm to remove remaining debris. Chlorophyll *a* concentration was then calculated using established protocols (Porra et al., 1989). Host protein concentrations were measured by the BCA method (Thermo Scientific), with bovine serum albumin used for standards. All absorbance measurements (chlorophyll and protein) were performed with a plate reader (FLUOstar Omega BMG labtech).

## Spectral Absorbance

For high and low light acclimated symbiont types, spectral absorbance measurements were performed as described in Enríquez et al. (2005) with reflectance ($R$) measured using a spectrometer (USB2000 Ocean Optics) and absorbance ($A$) calculated as $A = \log[1/R]$. Three traces were recorded per sample and a spectralon reflectance standard was utilized as a blank. Irradiance was provided by a full spectrum halogen light source (KL2500 LCD Schott). A running average was applied to each replicate trace prior to averaging. Significant differences among high and low light treatments were tested at absorbance wavelengths corresponding to those utilized by the chlorophyll *a* fluorometer (447, 505, 530, 597, 615, 625 nm).

## Statistical Analysis

Data-sets were tested for homogeneity of variance and normality of distribution using the Levene and Shapiro-Wilks tests, respectively. Data violating assumptions of normality and homoscedasticity ($p < 0.05$) were log transformed and retested. Significant differences in Fq′/Fm′ and $\sigma_{PSII}'$ values across all four symbiont types were tested by a one-way ANOVA (**Figures 2A,B**), followed by pairwise comparison across all four symbiont types with Tukey *post-hoc* analyses. Significant separation across symbiont types was assessed using an ANalyses Of SIMilarities test (ANOSIM) with 9,999 permutations. A *post-hoc* analysis of separation was not performed due to low replicate numbers ($n = 3$). Photo-physiological differences across all four symbiont types were visualized using non-metric multidimensional scaling (nMDS) on Euclidean distances after log (x+1) transformation (Ziegler et al., 2014). For high and low light acclimation comparisons, data were compared with a $T$-test with Bonferonni correction (**Figures 3–5**). Data comparison between the FIRe and Open-Sourced fluorometer was performed by a two-way analysis of variance (ANOVA) between light and symbiont type (**Figure 6**). As the primarily focus was to assess the similarity of responses detected between fluorimeters, significant effects were not followed up with *post-hoc* analyses. All statistical analyses were performed using R software with the "vegan," "car," "edgeR," "gplots," and "pgirmess" packages installed.

# RESULTS

## Effective Quantum Yield and Functional Absorption Cross Section in Different Symbionts

Effective quantum yield of PSII (Fq′/Fm′) varied across symbiont types and excitation wavelengths (**Figure 2A**). Symbiont type B1-b had between 15 and 23% higher yields than all others ($P = 0.0005$) at 505 nm. In addition, Fq′/Fm′ in anemones harboring B1-b was 30% greater than strain B1-a at 447 nm ($P = 0.02456$) and 24% higher than strains B1-a and A4-a at 530 nm ($P = 0.01324$) (**Figure 2A**). Symbiont strain A4-b had significantly greater (at least 42% higher) light acclimated absorption cross section values than the A4-a strain under all excitation wavelengths ($P < 0.034$) (**Figure 2B**). The A4-b symbiont strain had at least 28% greater light acclimated absorption cross section values than the two B1 strains when measured using 505, 597, and 615 nm excitation wavelengths ($P < 0.009$) (**Figure 2B**). Analysis of similarity (ANOSIM)

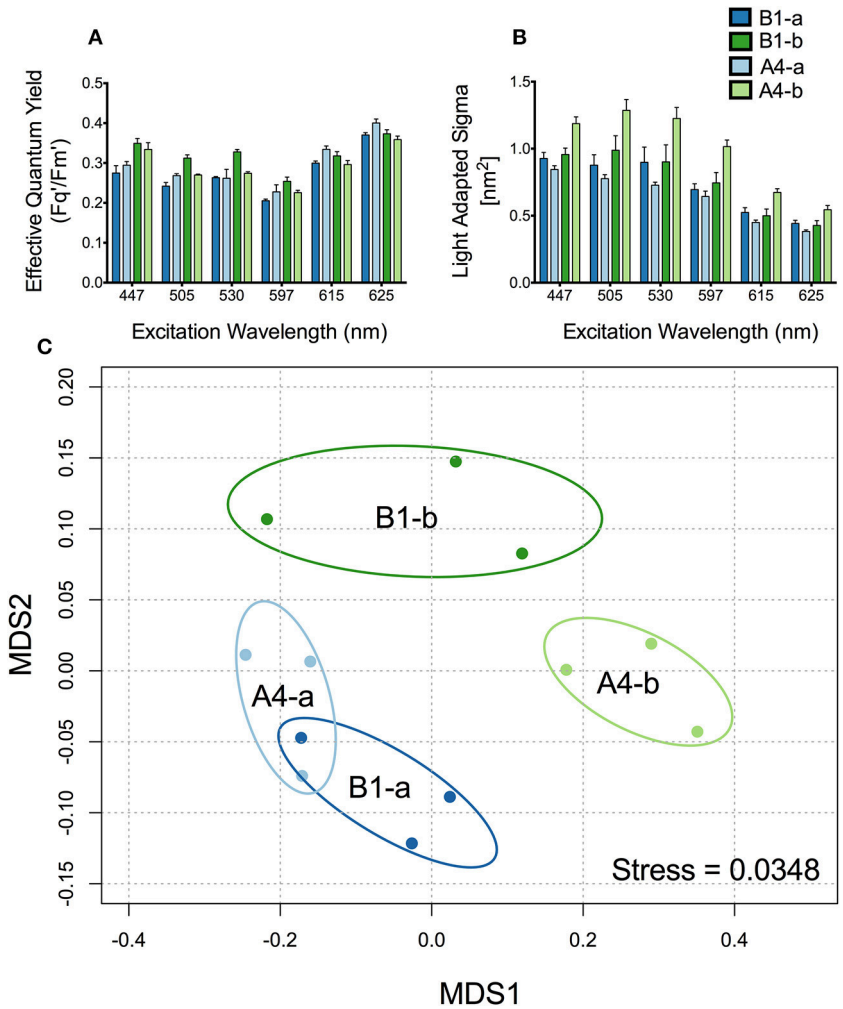


**FIGURE 2 |** Differences in fluorescence signature across symbiont types. **(A)** Effective quantum efficiency of PSII and **(B)** Light adapted absorption cross section ($\sigma_{PSII}$) for (dark blue) B1-a, (light blue) A4-a, (dark green) B1-b, and (light green) A4-b. Bars represent the mean and ±SE for low light adapted samples. **(C)** Principle components analysis using light adapted $\sigma_{PSII}$ and Fv'/Fm' for all four species. Ellipses represent a 95% confidence around the mean for each symbiont type.

confirmed a strong separation across symbiont types ($R$ = 0.7068, $P$ = 0.0014). Additionally, the MDS analysis shows that the direction of separation between the two Clade A symbionts differs from that of the two Clade B symbionts (**Figure 2C**). This is likely due to differences in Fq′/Fm′ driving the majority of separation between the two clade B symbionts (**Figure 2A**) whereas differences in the absorption cross section account for separation between clade A symbionts (**Figure 2B**).

## Spectrally Dependent Maximum Quantum Yield of PSII and Antennae Bed Quenching

The maximum quantum yield of PSII was statistically indistinguishable between low and high light acclimated animals harboring the A4-a symbiont strain at all excitation wavelengths (**Figure 3A**). However, Fv/Fm declined by 12–23% under high light acclimation across all six excitation wavelengths in anemones harboring the B1-a strain ($P$ = 0.02875, 0.0054, 0.0071, 0.0093, 0.0053, 0.0015 for 447, 505, 530, 597, 615, and 625 nm, respectively) (**Figure 3B**). There was a significant drop in the effective quantum yield in both sets of anemones, but only under the longer excitation wavelengths, with reductions for 615 nm ($P$ = 0.0121, 31% reduction) and 625 nm ($P$ = 0.0055, 27% reduction) for A4-a anemones and 597 nm ($P$ = 0.0088, 19% reduction), 615 nm ($P$ = 0.0140, 26% reduction) and 625 nm ($P$ = 0.0381, 25% reduction) for B1-a anemones (**Figures 3C,D**). High light acclimation in the A4-a anemones resulted in a significant decrease in non-photochemical quenching within the antennae bed at excitation wavelengths of 505 nm ($P$ = 0.0372, 40% reduction) and 530 nm ($P$ = 0.0385, 29% reduction) (**Figure 4A**). Non-significant reduction in antennae bed quenching was also observed using a 447 nm excitation wavelength, with a $P$-value of 0.05032 (**Figure 4A**), There were no significant changes in

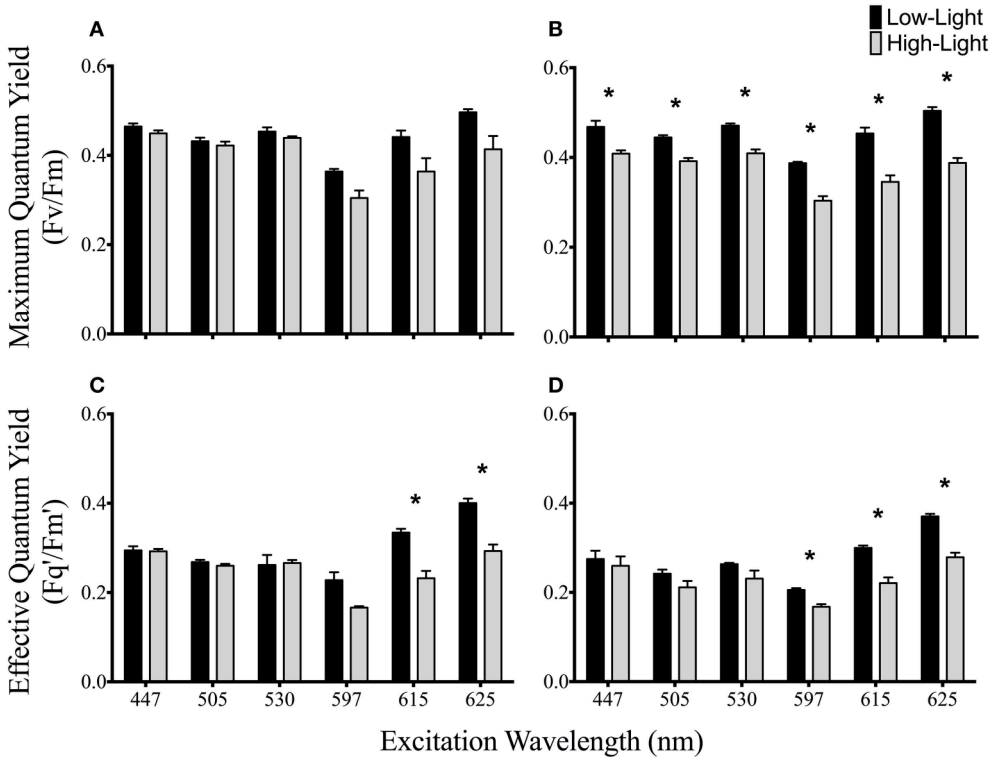


**FIGURE 3 |** Spectrally dependent maximum and effective quantum yields of PSII photochemistry in anemones photoacclimated to two light levels. Maximum quantum yields for high and low light acclimated **(A)** A4-a and **(B)** B1-a symbiont strains. High and low light acclimated effective quantum yields for **(C)** A4-a and **(D)** B1-a symbiont types. Dark bars represent low-light and gray bars represent high-light acclimated anemones. Error bars represent ±SE. Asterisks represent significant differences between low and high light conditions.

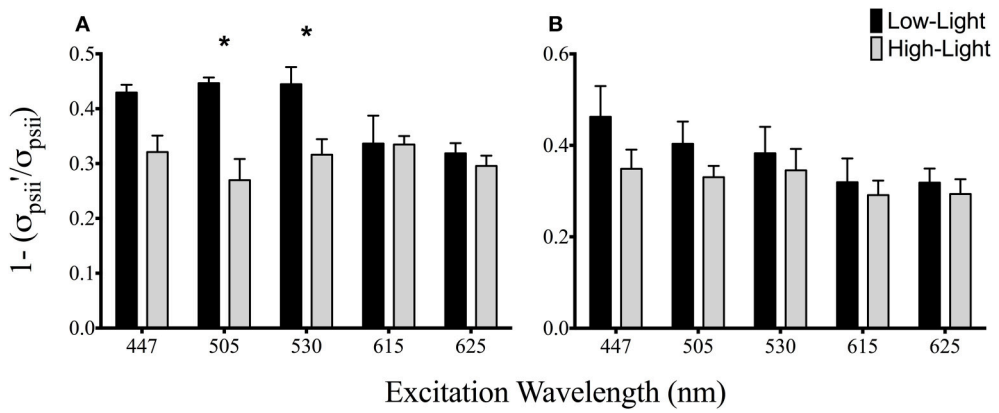


**FIGURE 4 |** Spectrally dependent antennae bed non-photochemical quenching for A4-a **(A)** and B1-a *Symbiodinium* **(B)**. Bars represent the mean and ±SE for (black) low and (gray) high light acclimated samples. Asterisks represent significant differences between low and high light conditions.

non-photochemical quenching in the antennae bed for the B1-a symbiont (**Figure 4B**). Excitation wavelength 597 nm was excluded from **Figure 4** as antennae bed quenching was very low as the wavelength has limited overlap with any major photopigments (Iglesias-Prieto et al., 1991; Iglesias-Prieto and Trench, 1997a).

## Absorption Spectra and Instrument Comparison

There were no differences between absorption spectra of high and low light acclimated anemones harboring the B1-a strain (**Figure 5B**). However, differences were observed for the A4-a strain, where absorption was significantly lower (57%)

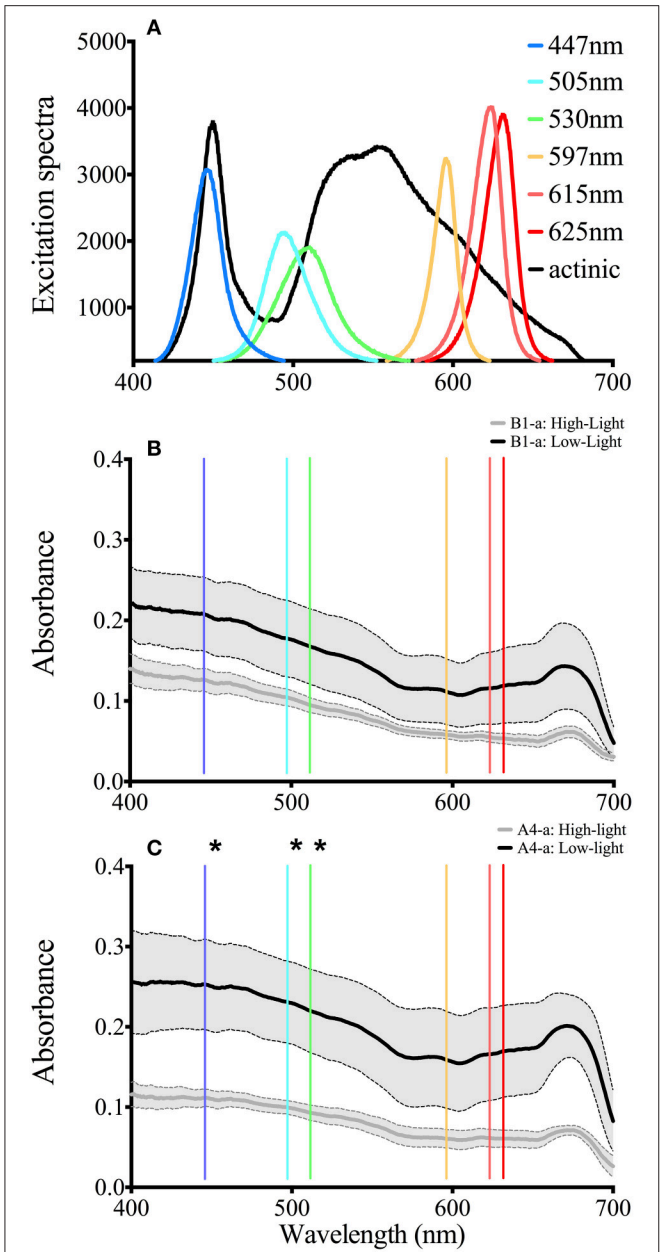


**FIGURE 5 |** LED output and whole anemone absorption Spectra. **(A)** Spectral characteristics for all six LED as well as the actinic light source. **(B)** Absorption spectra for the B1 symbiont under low (black) and high (gray) light conditions. **(C)** Absorption spectra for the B1 symbiont under low (black) and high (gray) light conditions. The solid line represents the average value and the gray area bounded by the dotted lines represent the standard deviation. Asterisks represent significant differences between low and high light conditions at the specific wavelengths.

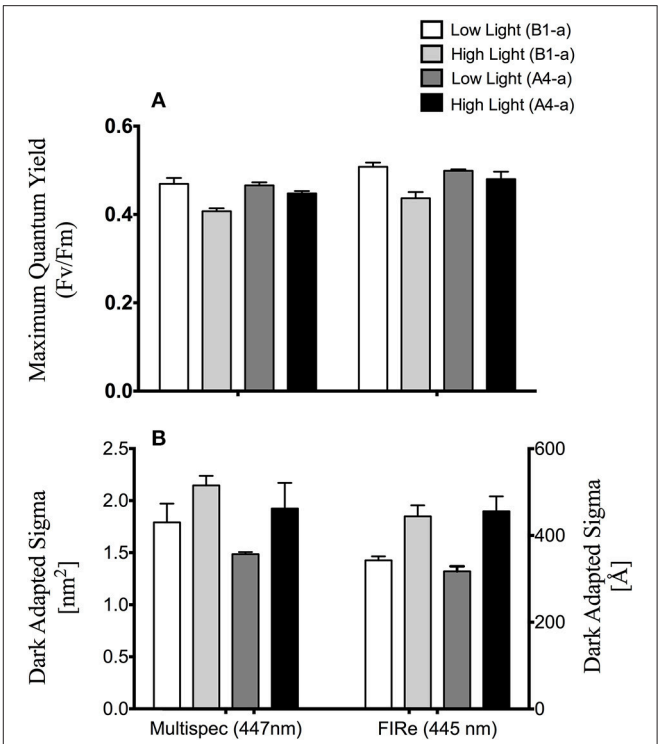


**FIGURE 6 |** Comparison of open source and FIRe fluorometers. **(A)** Average maximum quantum yield of PSII (Fv/Fm) and **(B)** functional absorption cross section of PSII ($\sigma_{PSII}$). Left and right axes reflect $\sigma_{PSII}$ units for the open-sourced and FIRe fluorometers respectively. Error bars represent ±SE.

at 447, 498, and 513 nm in high light acclimated animals (**Figure 5C**). When comparing the open-source instrument to the commercially produced FIRe fluorometer, similar absolute values, along with a significant reduction in Fv/Fm in response to high light was noted with both devices ($P = 0.0033$ and $P = 0.0057$, respectively; **Figure 6A**). However, using the open-sourced fluorometer, an interactive effect between symbiont type and light was also found ($P = 0.041$) as high-light reductions in Fv/Fm were only significant for the B1-a strain (**Figure 6A**). Although PSII functional absorption cross section is calculated in different units, both instruments detected similar total responses to high light acclimation where $\sigma_{PSII}$ was significantly higher under high light acclimation ($P = 0.0007$ for FIRe and $P = 0.0289$ for open-sourced (**Figure 6B**).

## Symbiont Cell Density, Volume, and Chlorophyll Content

Under low light conditions, cell density was 49–57% higher in B1-b as compared to the other symbiont strains ($P = 0.0099$). No significant differences in chlorophyll cell$^{-1}$ were observed across symbiont strains. However, symbiont strain B1-a had 49–76% higher cell volume ($P = 0.0066$) (**Table 2**) than the other three symbiont types. With respect to high-light acclimation, a two-way ANOVA revealed an interactive effect between light and symbiont type as B1-a cell volume significantly decreased by 28% under high light conditions, were as the A4-a symbiont did not change ($P = 0.0216$). Only chlorophyll content significantly declined by 73 and 59% under high light ($P = 0.0132$) within B1-a and A4-a symbiont strains, respectively (**Table 2**).

**TABLE 2 |** Symbiont physiology.

| Symbiont type | Light level | Cell density ($\mu$g host protein$^{-1}$) | Cell volume ($\mu m^{-3}$) | Chlorophyll (pg cell$^{-1}$) |
|---|---|---|---|---|
| B1-b | Low | 3453 ± 397 | 394 ± 34 | 5.18 ± 0.7 |
| A4-b | Low | 2226 ± 104 | 466 ± 39 | 4.44 ± 0.6 |
| B1-a | Low | 2196 ± 129 | 694 ± 63 | 4.17 ± 0.8 |
| A4-a | Low | 2317 ± 237 | 452 ± 51 | 4.10 ± 1.4 |
| B1-a | High | 2019 ± 125 | 502 ± 58 | 1.14 ± 0.5 |
| A4-a | High | 2070 ± 353 | 470 ± 21 | 1.69 ± 0.2 |

## DISCUSSION

Our results demonstrate wavelength dependent responses in both effective quantum yield and the functional absorption cross section of PSII across different symbionts. *Symbiodinium* have two major light harvesting complexes, the membrane bound Chla a-Chla $C_2$-peridinin-protein-complex (acpPC) and the soluble Peridinin-Chlorophyll Protein (PCP) complex, both of which absorb light predominantly between 400 and 550 nm (Iglesias-Prieto et al., 1991, 1993; Niedzwiedzki et al., 2013, 2014). Importantly, Iglesias-Prieto and Trench (1997b) demonstrated how the relative abundance of these different light harvesting compounds could vary across symbiont types growing in culture and/or with respect to high vs. low light acclimation. This was further refined by Hennige et al. (2009) whom used high performance liquid chromatography (HPLC) to compare the relative photopigment concentrations across eight different symbiont types. Such differences may give rise to the spectrally dependent differences across algal species observed here (**Figure 2**). Data from this study largely agree with previous work that used a commercially available multi-spectral pulse amplitude modulation (PAM) fluorometer with a symbiotic coral, that also documented clear wavelength dependencies in *Symbiodinium* photochemical activity (Szabó et al., 2014). In particular, the A4-b (strain: KLAp2) symbiont displayed a higher absolute PSII functional absorption cross section in the light activated state ($\sigma_{PSII'}$) relative to the other symbiotic algae, and similar to the results of Szabó et al. (2014) (albeit in their dark acclimated samples), higher ($\sigma_{PSII'}$) in lower excitation wavelengths (447–530 nm) which then decreased toward red excitation (**Figure 2A**). In contrast, the light acclimated PSII absorption cross section of the A4-a symbiont steadily decreased as excitation light moved from the blue to the red spectrum. Because the photopigments diadinoxanthin and peridinin have peak absorbance values near 505 and 530 nm, respectively, such divisions in $\sigma_{PSII'}$ could be driven by different levels of Chl *a*:diadinoxanthin or Chl *a*:peridinin ratios as well as light harvesting protein content. The decline in functional absorption cross section toward the red excitation spectrum is also naturally due to lower light harvesting complex absorption in the higher wavelength range. In corals, this also correlates to a higher scalar irradiance at higher wavelengths (Wangpraseurt et al., 2012), however, it is not known if a similar irradiance pattern exists in a symbiotic sea anemone that lacks a calcium carbonate skeleton.

The significant drop in chlorophyll *a* concentration in the high light acclimated A4-a and B1-a symbionts is a common photoacclimation response which significantly decrease the amount of light captured by the cell, thereby reducing the potential for excess excitation energy under high irradiance levels. Photoacclimation in *Symbiodinium* has been documented among a number of different species and the overall response is well-understood (Iglesias-Prieto and Trench, 1994, 1997b; Hennige et al., 2009; Finney et al., 2010). Similar to that observed during stress conditions, total organism absorbance may also decline, as symbionts reduce the amount of light that is absorbed and channeled toward photosynthesis (Rodriguez-Román et al., 2006; Hoadley et al., 2016). Although absorbance decreased in the high light acclimated anemones harboring the A4-a alga, there was no significant change in absorbance between the two acclimation light levels for the anemones harboring the B1-a symbiont. Despite the decline in Chl *a* cell$^{-1}$ in the high light acclimated B1-a, this lower absorption difference may have been due, in part, to the alga cell size which also declined during high light acclimation, thus chlorophyll cellular volume$^{-1}$ and pigment packaging may have remained similar across the two light levels.

Interestingly, acclimation to high light conditions reduced Fq′/Fm′ in both symbiont types, but only when excited with red spectrum (597–625 nm) wavelengths. Because photoprotective pigments such as xanthophylls do not absorb at these wavelengths, it is possible that the observed reductions in Fq′/Fm′ are indicative of decoupling between PSII reaction centers and light harvesting proteins. Apart from this reduction in Fq′/Fm′, the two holobionts showed marked photochemical differences in their patterns of photoacclimation, as the B1-a alga displayed a consistent down-regulation of functional PSII reaction centers (i.e., significant decline in Fv/Fm) (**Figure 3B**), while the A4-a symbiont reduced overall absorbance more and displayed a reduction in antennae-based non-photochemical quenching (**Figure 4A**) while Fv/Fm remained stable (**Figure 3A**). Under high light acclimation, microalgae tend to increase photo-protective mechanisms such as antennae-based non-photochemical quenching (Suggett et al., 2007). The reductions in non-photochemical quenching within the antennae bed observed for A4-a may possibly reflect a difference in optics associated with living inside the host anemone as opposed to free-living as is the case for most microalgal light acclimation studies. Coral tissues contain numerous fluorescent proteins which can substantially change the perceived light field for *in situ* symbionts (Dove, 2004). These host derived proteins may also differ across light and temperature gradients thus potentially also influencing symbiont response to elevated light conditions (Salih et al., 2000). Current efforts in understanding the miroenvironments in which *Symbiodinium* live (Wangpraseurt et al., 2012; Lichtenberg et al., 2016) are critical for improving our knowledge of coral/algal photoprotective mechanisms.

To ground-truth our fluorometer, we compared measurements of the same samples against a single excitation (peak 447 nm) Fluorescence Induction and Relaxation (FIRe) fluorometer (Satlantic Inc.). Both systems reported similar Fv/Fm values and overall trends in response to low and high light

acclimation (**Figure 6**). Likewise, a similar response in functional absorption cross section was noted for both instruments, as high light acclimation led to elevated $\sigma_{PSII}$ values. The slight reduction in Fv/Fm in the B1-a alga under high light acclimation noted with both systems is consistent with previously published work with most cultured *Symbiodinium* and reef corals (Lesser and Gorbunov, 2001; Hennige et al., 2009), however, the rise in $\sigma_{PSII}$ under high light is not as common, and $\sigma_{PSII}$ in cultured *Symbiodinium* tend to decrease slightly under high light (see Hennige et al., 2009 for one exception to this in a cultured F2 alga).

It is interesting to note that while the symbiont-anemone combinations used in this study contained a similar symbiont density and Chl. *a* algal cell$^{-1}$ (**Table 2**), multispectral active chlorophyll fluorescence revealed clear differences in symbiont photochemical efficiency that would be missed by a conventional fluorometer using a single wavelength band excitation light source. Importantly, symbiont density was normalized to the quantity of total soluble animal protein, and this does not account for possible structural differences between these two anemone populations, symbiont distributions across anemone location (e.g., tentacles vs. oral disc), or light absorbing animal pigments, all of which could significantly alter the photosynthetically usable radiation (PUR) in these animals further.

Different algal populations were separated by their light acclimated photochemical patterns (**Figure 2C**), but were not resolvable from dark acclimated samples alone (not shown). Spectrally dependent differences in algal photochemistry can not only provide more detail of photochemical differences within a single symbiosis, and also may potentially be a powerful tool for resolving genetically (and functionally) different *Symbiodinium* populations across diverse cnidarian hosts, including reef building corals. These results, while limited in scope, are similar to those of a more extensive study by Suggett et al. (2015) that examined 18 genetically distinct cultured *Symbiodinium* isolates with a single waveband excitation (peak excitation, 450 nm) fast repetition rate fluorometer. Specifically, that work noted that different phylotypes of *Symbiodinium* could be grouped into particular clusters based on the balance of how symbionts used the fraction of open PSII reaction centers (i.e., photochemical quenching or [1-*C*] vs. non-photochemical quenching [1-*Q*]).

There is a growing interest in the field of plant biology to better characterize genomic expression by characterizing specific phenotypic traits in a given environment, also known as phenomics (Furbank and Tester, 2011). Similar to the desire to link genomics to plant function and favorable agricultural traits, there is a growing need to characterize specific physiological traits of symbiotic reef building corals to their environment (Madin et al., 2016; Warner and Suggett, 2016). Active chlorophyll fluorescence is one such tool that has the potential to allow for rapid high throughput screening of photochemical response to different environmental conditions.

This work suggests that low-cost multispectral chlorophyll *a* fluorescence may prove useful in delineating functional traits as well as groups of different symbionts. Open source hardware and software platforms are becoming increasingly popular within the research community as their ease of use and low cost promotes high levels of customization for specific applications and a broad user base that reaches beyond traditional academic research. For example, the MultspeQ is a recently developed fluorometer designed to promote greater utilization across both scientific and community users interested in assessing terrestrial plant physiological responses via a phenomics-based approach (Kuhlgert et al., 2016). By utilizing chlorophyll fluorescence and absorbance based parameters, it is designed to provide a common platform to compare the photochemical traits of plant species worldwide. This device is relatively low cost, in part, due to the utilization and promotion of open access hardware and software platforms. The advantage of a greater user base also allows for higher level interpretation and analysis of the collected data. Although this current study does not offer a fully developed product for other users, it serves as an example of the type of research that can be achieved through the integration of open source platforms with specific research questions in mind and relatively inexpensive hardware. As more advanced hardware platforms adopt the open source concept, it is possible that even more sophisticated and low-cost instrumentation will become more accessible to a larger community of scientific and public community users interested in monitoring the physiological stability of algal-invertebrate symbioses as well.

In conclusion, spectrally dependent characteristics of symbiont photochemistry were effectively quantified using a multispectral chlorophyll-*a* fluorometer. It is likely that the spectrally dependent characteristics observed here correlate with differences in photopigment abundance across symbiont types as has been previously shown using immunoblot and HPLC analyses (Iglesias-Prieto et al., 1991; Iglesias-Prieto and Trench, 1997b; Hennige et al., 2009). With respect to symbiont types A4-a and B1-a, spectrally resolved Fv/Fm and $\sigma_{PSII}$ values revealed additional changes in response to high-light acclimation that would not be possible if using more conventional active chlorophyll-*a* fluorometers with a single excitation wavelength centered at 450 nm. Importantly, these spectrally resolved fluorescence measurements were made using a custom built fluorometer using open source hardware and software platforms. Our work serves as an example of the potential for open source platforms to be utilized to construct purpose built and relatively low-cost instruments.

## AUTHOR CONTRIBUTIONS

All authors listed have made a substantial, direct and intellectual contribution to the work, and approved it for publication.

## ACKNOWLEDGMENTS

This project was supported by funding from the National Science Foundation (awards 1316055 and 1258065 to MW).

## REFERENCES


Baker, A. C. (2003). Flexibility and specificity in coral-algal symbiosis: diversity, ecology, and biogeography of *Symbiodinium*. *Annu. Rev. Ecol. Evol. Syst.* 34, 661–689. doi: 10.1146/annurev.ecolsys.34.011802.132417

Dove, S. (2004). Scleractinian corals with photoprotective host pigments are hypersensitive to thermal bleaching. *Mar. Ecol. Prog. Ser.* 272, 99–116. doi: 10.3354/meps272099

Enríquez, S., Méndez, E. R., and Iglesias-Prieto, R. (2005). Multiple scattering on coral skeletons enhances light absorption by symbiotic algae. *Limnol. Oceanogr.* 50, 1025–1032. doi: 10.4319/lo.2005.50.4.1025

Finney, J. C., Pettay, D. T., Sampayo, E. M., Warner, M. E., Oxenford, H. A., and LaJeunesse, T. C. (2010). The relative significance of host-habitat, depth, and geography on the ecology, endemism, and speciation of coral endosymbionts in the genus *Symbiodinium*. *Microb. Ecol.* 60, 250–263. doi: 10.1007/s00248-010-9681-y

Furbank, R. T., and Tester, M. (2011). Phenomics–technologies to relieve the phenotyping bottleneck. *Trends Plant Sci.* 16, 635–644. doi: 10.1016/j.tplants.2011.09.005

Gorbunov, M. Y., Kolber, Z. S., Lesser, M., and Falkowski, P. G. (2001). Photosynthesis and photoprotection in symbiotic corals. *Limnol. Oceanogr.* 46, 75–85. doi: 10.4319/lo.2001.46.1.0075

Hawkins, T. D., Hagemeyer, J., and Warner, M. E. (2016). Temperature moderates the infectiousness of two conspecific Symbiodinium strains isolated from the same host population. *Environ. Microbiol.* 18, 5204–5217. doi: 10.1111/1462-2920.13535

Hennige, S. J., Suggett, D. J., Warner, M. E., McDougall, K. E., and Smith, D. J. (2009). Photobiology of *Symbiodinium* revisited: bio-physical and bio-optical signatures. *Coral Reefs* 28, 179–195. doi: 10.1007/s00338-008-0444-x

Hoadley, K. D., Pettay, D. T., Dodge, D., and Warner, M. E. (2016). Contrasting physiological plasticity in response to environmental stress within different cnidarians and their respective symbionts. *Coral Reefs* 35, 529–542. doi: 10.1007/s00338-016-1404-5

Hochberg, E. J., Apprill, A. M., Atkinson, M. J., and Bidigare, R. R. (2006). Bio-optical modeling of photosynthetic pigments in corals. *Coral Reefs* 25, 99–109. doi: 10.1007/s00338-005-0071-8

Iglesias-Prieto, R., Beltran, V. H., LaJeunesse, T. C., Reyes-Bonilla, H., and Thome, P. E. (2004). Different algal symbionts explain the vertical distribution of dominant reef corals in the eastern Pacific. *Proc. R. Soc. Lond. B.* 271, 1757–1763. doi: 10.1098/rspb.2004.2757

Iglesias-Prieto, R., Govind, N., and Trench, R. (1991). Apoprotein composition and spectroscopic characterization of the water- soluble peridinin-chlorophyll a-proteins from three symbiotic dinoflagellates. *Philos. Trans. R. Soc. Lond. B.* 246, 275–283. doi: 10.1098/rspb.1991.0155

Iglesias-Prieto, R., Govind, N., and Trench, R. (1993). Isolation and characterization of three membrane-bound chlorophyll-protein complexes from four dinoflagellate species. *Philos. Trans. R. Soc. Lond. B*. 340, 381–392. doi: 10.1098/rstb.1993.0080

Iglesias-Prieto, R., and Trench, R. (1994). Acclimation and adaptation to irradiance in symbiotic dinoflagellates. I. Responses of the photosynthetic unit to changes in photon flux density. *Mar. Ecol. Prog. Ser.* 113, 163–175. doi: 10.3354/meps113163

Iglesias-Prieto, R., and Trench, R. (1997a). "Photoadaptation, photoacclimation and niche diversification in invertebrate- dinoflagellate symbioses," in *Proceedings of the 8th International Coral Reef Symposium*, eds H. Lessios and I. Macintyre (Balboa: Smithsonian Tropical Research Institute), 1319–1324.

Iglesias-Prieto, R., and Trench, R. K. (1997b). Acclimation and adaptation to irradiance in symbiotic dinoflagellates. II. Response of chlorophyll-protein complexes to different photon-flux densities. *Mar. Biol.* 130, 23–33. doi: 10.1007/s002270050221

Kemp, D. W., Cook, C. B., LaJeunesse, T. C., and Brooks, W. R. (2006). A comparison of the thermal bleaching responses of the zoanthid *Palythoa caribaeorum* from three geographically different regions in south Florida. *J. Exp. Mar. Biol. Ecol.* 335, 266–276. doi: 10.1016/j.jembe.2006.03.017

Kolber, Z., and Falkowski, P. (1998). Measurements of variable chlorophyll fluorescence using fast repetition rate techniques: defining methodology and experimental protocols. *Biochim. Biophys.* 1367, 88–107. doi: 10.1016/S0005-2728(98)00135-2

Kuhlgert, S., Austic, G., and Zegarac, R. (2016). MultispeQ Beta: a tool for large-scale plant phenotyping connected to the open PhotosynQ network. *R. Soc. Open Sci.* 3:160592. doi: 10.1098/rsos.160592

LaJeunesse, T. C. (2001). Investigating the biodiversity, ecology, and phylogeny of endosymbiotic dinoflagellates in the genus *Symbiodinium* using the ITS region: in search of a "species" level marker. *J. Phycol.* 37, 866–880. doi: 10.1046/j.1529-8817.2001.01031.x

LaJeunesse, T. C., Smith, R. T., Finney, J., and Oxenford, H. (2009). Outbreak and persistence of opportunistic symbiotic dinoflagellates during the 2005 Caribbean mass coral 'bleaching' event. *Proc. R. Soc. B.* 276, 4139–4148. doi: 10.1098/rspb.2009.1405

LaJeunesse, T., and Trench, R. (2000). Biogeography of two species of Symbiodinium (Freudenthal) inhabiting the intertidal sea anemone *Anthopleura elegantissima* (Brandt). *Biol. Bull.* 199, 126–134. doi: 10.2307/1542872

Lesser, M. P., and Gorbunov, M. Y. (2001). Diurnal and bathymetric changes in chlorophyll fluorescence yields of reef corals measured *in situ* with a fast repetition rate fluorometer. *Mar. Ecol. Prog. Ser.* 212, 69–77. doi: 10.3354/meps212069

Lichtenberg, M., Larkum, A. W. D., and Kühl, M. (2016). Photosynthetic acclimation of Symbiodinium in hospite depends on vertical position in the tissue of the scleractinian coral *Montastrea curta*. *Front. Microbiol.* 7:230. doi: 10.3389/fmicb.2016.00230

Madin, J. S., Hoogenboom, M. O., and Connolly, S. R. (2016). A trait-based approach to advance coral reef science. *Trends Ecol. Evol.* 31, 419–428. doi: 10.1016/j.tree.2016.02.012

Muscatine, L. (1990). "The role of symbiotic algae in carbon and energy flux in reef corals," in *Ecosystems of the World: Coral Reefs,* ed Z. Dubinsky (Amsterdam: Elsevier), 75–87.

Muscatine, L., Falkowski, P., Porter, J., and Dubinsky, Z. (1984). Fate of photosynthetic fixed carbon in light and shade-adapted colonies of the symbiotic coral *Stylophora pistillata*. *Proc R. Soc. Lond. B*. 222, 181–202. doi: 10.1098/rspb.1984.0058

Niedzwiedzki, D. M., Jiang, J., and Lo, C. S. (2014). Spectroscopic properties of the Chlorophyll a–Chlorophyll c2–Peridinin-Protein-Complex (acpPC) from the coral symbiotic dinoflagellate Symbiodinium. *Photosyn. Res.* 120, 125–139. doi: 10.1007/s11120-013-9794-5

Niedzwiedzki, D. M., Jiang, J., Lo, C. S., and Blankenship, R. E. (2013). Low-temperature spectroscopic properties of the peridinin–chlorophyll a–protein (PCP) complex from the coral symbiotic dinoflagellate Symbiodinium. *J. Phys. Chem. B*. 117, 11091–11099. doi: 10.1021/jp401022u

Ortiz, J. C., González-Rivero, M., and Mumby, P. J. (2012). Can a thermally tolerant symbiont improve the future of Caribbean coral reefs? *Global Change Biol*. 19, 273–281. doi: 10.1111/gcb.12027

Porra, R. J., Thompson, W. A., and Kriedemann, P. E. (1989). Determination of accurate extinction coefficients and simultaneous equations for assaying chlorophylls *a* and *b* extracted with four different solvents: verification of the concentration of chlorophyll standards by atomic absorption spectroscopy. *Biochim. Biophys. Acta* 975, 384–394. doi: 10.1016/S0005-2728(89)80347-0

Rodriguez-Román, A., Hernández-Pech, X., Thome, P. E., Enriquez, S., and Iglesias-Prieto, R. (2006). Photosynthesis and light utilization in the Caribbean coral *Montastraea faveolata* recovering from a bleaching event. *Limnol. Oceanogr.* 51, 2702–2710. doi: 10.4319/lo.2006.51.6.2702

Salih, A., Larkum, A., Cox, G., Kühl, M., and Hoegh-Guldberg, O. (2000). Fluorescent pigments in corals are photoprotective. *Nature* 408, 850–853. doi: 10.1038/35048564

Silverstein, R. N., Correa, A. M. S., LaJeunesse, T. C., and Baker, A. C. (2011). Novel algal symbiont (*Symbiodinium* spp.) diversity in reef corals of Western Australia. *Mar. Ecol. Prog Ser*. 422, 63–75. doi: 10.3354/meps08934

Suggett, D. J., Goyen, S., Evenhuis, C., Szabó, M., Pettay, D. T., Warner, M. E., et al. (2015). Functional diversity of photobiological traits within the genus Symbiodinium appears to be governed by the interaction of cell size with cladal designation. *New Phytol.* 208, 370–381. doi: 10.1111/nph.13483

Suggett, D. J., Le Floc'H, E., Harris, G. N., Leonardos, N., and Geider, R. J. (2007). Different strategies of photoacclimation by two strains of *Emiliania huxleyi* (Haptophyta). *J. Phycol.* 43, 1209–1222. doi: 10.1111/j.1529-8817.2007.00406.x

Suggett, D. J., Oxborough, K., Baker, N. R., MacIntyre, H. L., Kana, T. M., and Geider, R. J. (2003). Fast repetition rate and pulse amplitude modulation

chlorophyll a fluorescence measurements for assessment of photosynthetic electron transport in marine phytoplankton. *Eur. J. Phycol.* 38, 371–384. doi: 10.1080/09670260310001612655

Sunagawa, S., Wilson, E. C., Thaler, M., Smith, M. L., Caruso, C., Pringle, J. R., et al. (2009). Generation and analysis of transcriptomic resources for a model system on the rise: the sea anemone *Aiptasia pallida* and its dinoflagellate endosymbiont. *BMC Genomics* 10:258. doi: 10.1186/1471-2164-10-258

Szabó, M., Wangpraseurt, D., and Tamburic, B. (2014). Effective light absorption and absolute electron transport rates in the coral *Pocillopora damicornis*. *Plant Physiol. Biochem.* 83, 159–167. doi: 10.1016/j.plaphy.2014.07.015

Wangpraseurt, D., Larkum, A. W. D., Ralph, P. J., and Kuhl, M. (2012). Light gradients and optical microniches in coral tissues. *Front. Microbiol.* 3:316. doi: 10.3389/fmicb.2012.00316

Wangpraseurt, D., Tamburic, B., Szabó, M., and Suggett, D. (2014). Spectral effects on Symbiodinium photobiology studied with a programmable light engine. *PLoS ONE* 9:e112809. doi: 10.1371/journal.pone.0112809

Warner, M. E., and Suggett, D. J. (2016). "The photobiology of *Symbiodinium* spp.: linking physiological diversity to the implications of stress and resilience," in *The Cnidaria, Past, Present and Future*, eds S. Goffredo and Z. Dubinsky (Cham: Springer), 489–509.

Zhang, Z., Green, B. R., and Cavalier-Smith, T. (2000). Phylogeny of ultra-rapidly evolving dinoflagellate chloroplast genes: a possible common origin for sporozoan and dinoflagellate plastids. *J. Mol. Evol.* 51, 26–40. doi: 10.1007/s002390010064

Ziegler, M., Roder, C. M., Büchel, C., and Voolstra, C. R. (2014). Limits to physiological plasticity of the coral Pocillopora verrucosa from the central Red Sea. *Coral Reefs* 33, 1115–1129. doi: 10.1007/s00338-014-1192-8

**Conflict of Interest Statement:** The authors declare that the research was conducted in the absence of any commercial or financial relationships that could be construed as a potential conflict of interest.